

SEA ICE DETECTION IN THE SEA OF OKHOTSK USING PALSAR POLARIMETRIC DATA

PI No. 205

Hiroyuki Wakabayashi¹, Shoji Sakai¹, Kazuki Nakamura², and Fumihiko Nishio³

¹ College of Engineering, Nihon University, 1 Nakagawara, Tokusada, Tamura, Koriyama 963-8642 Japan, E-mail: hwaka@cs.ce.nihon-u.ac.jp

² National Institute of Advanced Industrial Science and Technology, AIST Tsukuba Central 7, 1-1-1 Higashi, Tsukuba, Ibaraki, 305-8567 Japan, E-mail: nakamura-kazuki@aist.go.jp

³ Center for Environmental Remote Sensing, Chiba University, 1-33 Yayoicho, Inage-ku, Chiba 263-8522 Japan, E-mail: fnishio@faculty.chiba-u.jp

1. INTRODUCTION

An extent of sea ice is related to local as well as global climate change, because sea ice acts as an insulator between air and seawater. It is very important to monitor an extent and volume of sea ice in order to understand global climate changes [1]. Since the microwave remote sensing is expected to play an important role in monitoring sea ice in cryosphere due to its all weather observation capabilities, the data from microwave radiometer are mainly used in sea ice monitoring so far. However, the microwave radiometer data have been used limitedly in the Sea of Okhotsk, because the spatial resolution is not good enough for regional monitoring of sea ice, especially in the area close to land-sea boundary. In addition, since NASA team algorithm is using 89GHz data to estimate sea ice concentration, it produces some error in clouded area. Considering the above-mentioned problems, if the SAR data can be applied to monitor sea ice in the Sea of Okhotsk, the spatial resolution problem will be solved and greatly contributed to operational sea ice monitoring.

The objective of this research is mainly in detecting sea ice from Phased-Array L-band SAR (PALSAR) polarimetric data. This paper shows the results of estimating sea ice concentration from PALSAR polarimetric data acquired from 2008 to 2010. The AMSR-E sea ice concentration and MODIS data were used to verify the results of sea ice detected by PALSAR data.

2. TEST SITE

It is well known that the Sea of Okhotsk is located in the most southerly region of the Northern Hemisphere where the sea ice exists, because the seawater has relatively low salinity and its freezing temperature is high in this region. Sea ice in this area exists only in wintertime and its average thickness is relatively thin comparing with the Arctic Sea. The accuracy of sea ice concentration estimated from the

microwave radiometer data is relatively low, because lands and islands surround this region.

Our test site is located between Hokkaido and Sakhalin islands in the southern region of the Sea of Okhotsk. Most of sea ice found in this region has the thickness less than one meter. Based on ice core structure analysis, it is suggested that the dynamical ice growth process under turbulent conditions such as frazil ice formation and floe accumulation are the dominant contributors to thick ice growth in this region [2]. Our test site for this analysis is located southern region of the Sea of Okhotsk, and shown in Fig. 1.



Fig. 1 Location of our test site.

3. SATELLITE DATA

The Japan Aerospace Exploration Agency (JAXA) launched PALSAR aboard the Advanced Land Observing Satellite (ALOS) in January 2006. Although the ALOS has

been observing the Sea of Okhotsk more than three years, there were a few PALSAR polarimetric data acquired in the Sea of Okhotsk in the sea ice growing season so far, because of the conflict with Japan Coast Guard ScanSAR requirements. Four polarimetric observations were finally conducted in our test site during three consecutive wintering periods from 2008 to 2010.

We also used AMSR-E data in order to evaluate our method to estimate sea ice concentration from polarimetric SAR data. AMSR-E is capable to observe six frequency bands with wide swath. The observed data are used to estimate sea ice concentration in the Arctic and Antarctic regions. The sea ice concentration derived from AMSR-E data are provided by the National Snow and Ice Data Center (NSIDC) and Earth Observation Research Center (EORC) in routine basis.

In order to verify the high-resolution sea ice area detected by PALSAR data, MODIS data acquired in 2010 were used. The albedo was calculated from MODIS visible channels and the threshold was applied to detect the sea ice area. The sea ice area map that has a spatial resolution of 500 m was created. The data used in this research are summarized in Table 1.

Table 1. List of data in this analysis

Satellite/Sensor	Observation date	Process Level
ALOS/PALSAR	2008/02/15	Level 1.1 Full polarimetry (JAXA/EORC)
	2008/02/17	
	2009/02/17	
	2010/02/20	
Aqua/AMSR-E	2008/02/15	Level 2 Sea ice concentration (JAXA/EORC)
	2008/02/17	
	2009/02/17	
	2010/02/20	
Aqua/MODIS	2010/02/20	Level 1B (NSIDC)

4. ESTIMATION OF SEA ICE CONCENTRATION FROM POLARIMETRIC SAR DATA

4.1 Problems in sea ice detection by SAR data

Problems in estimating sea ice concentration by using SAR data are clarified in this section. The backscattering coefficient of open water depends on water surface roughness, which is related to sea surface wind velocity. After the water starts freezing, the backscattering coefficient decreases until the thickness reaches several centimeters. This is due to the decrease of dielectric constant of ice

surface related to ice growth. Since the surface roughness increases as the ice grows, which is due to existence of frost flower and so on, the backscattering coefficient increases until the thickness reaches 20 centimeters. The backscattering coefficient decreases again after the ice thickness increases over 20 centimeters [3].

Threshold of backscattering coefficient must be used for sea ice detection, when the single polarization SAR data are used. The backscattering coefficients for both sea ice and open water change as described above, it is generally difficult to set a threshold value to classify sea ice and open water.

4.2 Scattering entropy

In order to solve problems in detecting sea ice area by SAR data, we propose a new method to estimate sea ice concentration from PALSAR polarimetric data, which is based on the result of our past research. Our previous research showed that the scattering entropy of open water gives consistently low value in wide range of incidence angle, because the surface scattering is dominant in open water. On the contrary, the scattering entropy of various sea ices gives higher value than that of open water [4]. Therefore, we propose that the scattering entropy can be used to distinguish sea ice from open water.

The scattering entropy is calculated from eigenvalues of covariance or coherence matrix of the observed scattering matrix. The scattering entropy is calculated as follows,

$$H = \sum_{i=1}^3 -P_i \log_3 P_i \quad (1)$$

where P_i is i -th. normalized eigenvalues. Each eigenvalue is related to the ratio of odd scattering, even scattering, and diffuse scattering of total scattering power [5]. The scattering entropy is recognized as an index of the randomness of scattering mechanisms. When the scattering is dominated by single scattering mechanism, the scattering entropy shows low value. The maximum entropy is one.

The scattering entropy for sea ice, which depends on its surface roughness and thickness, usually takes higher value than that of open water [4]. This means that surface scattering does not dominate in the total scattering. In return, since the dominant scattering is surface scattering for open water in any case of surface conditions, we suspected that we can set a threshold of the scattering entropy to classify the sea ice and the open water.

4.3 Threshold of the scattering entropy to detect sea ice

In order to determine a threshold for detecting open water from scattering entropy data, we compared the values of scattering entropy for various sea ice types with AMSR-E data. Based on the results of similar research, in which AMSR-E sea ice concentration was compare with RADARSAT-1 and MODIS imagery [6], we tried to

determine the threshold of scattering entropy to detect sea ice area.

The followings are the procedure for PALSAR data pre-processing in this research.

- (1) Calculate the scattering entropy in the area of 8 by 4 samples of PALSAR Level 1.1 data. The scattering entropy image is scaled 0 to 255 ranges, which corresponds 0 to 1.
- (2) Transform the scattering entropy image onto UTM coordinate with the pixel spacing of 25 by 25 meters. The resampling method applied to this conversion is Bilinear resampling.
- (3) Combine 6 or 7 images between Sakhalin and Hokkaido islands to make a mosaic image.
- (4) By using the land and ocean boundary, PALSAR data and AMSR-E data are transformed into the same coordinate. In this operation, the PALSAR data are averaged within the size of AMSR-E data.

Fig. 2 shows a scatter plot of the scattering entropy and AMSR-E sea ice concentration. As the result of regression analysis, we found that the threshold of the scattering entropy should be 0.15, which corresponds 0 % of sea ice concentration in the AMSR-E data. The derived threshold is consistent with the result of the scattering entropy in the incidence angle range from 20 to 30 degrees in our past research [4].

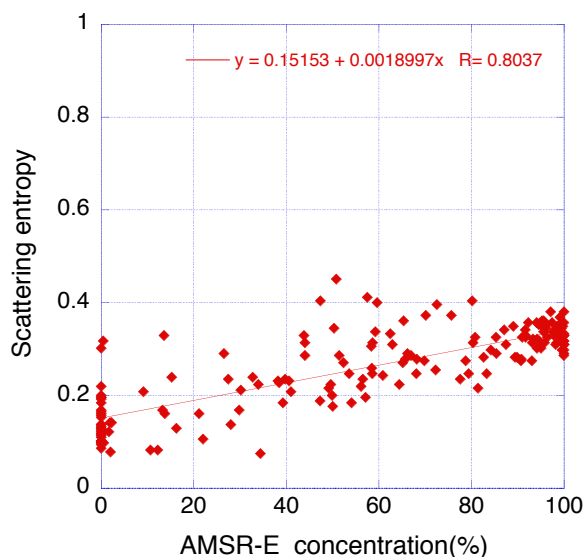


Fig. 2 Scatter plot of the scattering entropy and AMSR-E sea ice concentration.

4.4 Sea ice concentration derived from PALSAR polarimetric data

A binary image, which is created by setting the threshold value for the PALSAR entropy image, gives us a distribution map of sea ice with the pixel spacing of 25 by 25 meters. Fig. 3 shows the flow of estimation for PALSAR sea ice concentration. The SRTM-3 DEM data are used in

order to mask the land area, and sea ice concentration is calculated based on the ratio of sea ice area to total area. Fig. 4 shows an example of sea ice concentration estimated from PALSAR data as compared with AMSR-E sea ice concentration.

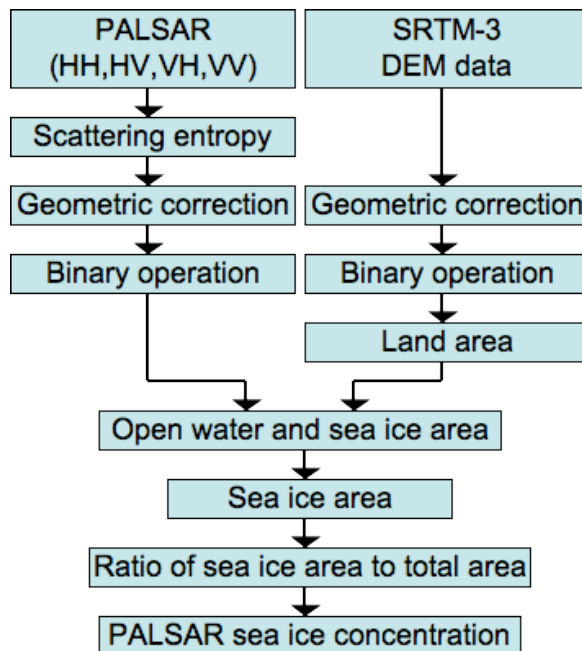


Fig. 3 Estimation flow of PALSAR sea ice concentration.

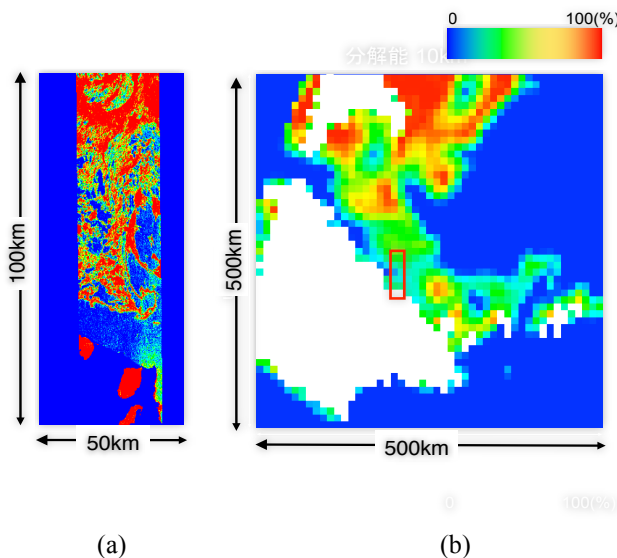


Fig. 4 Example of high-resolution sea ice concentration derived from PALSAR data acquired on Feb 20.2010. AMSR-E sea ice concentration on the same day is shown in comparison. (a) PALSAR sea ice concentration (Pixel spacing 250m) (b) AMSR-E sea ice concentration (Pixel spacing 10.0km).

5. DISCUSSION

5.1 Comparison between PALSAR sea ice concentration and AMSR-E sea ice concentration

In order to verify our method for deriving sea ice concentration from PALSAR data, we used the AMSR-E sea ice concentration data, which are distributed routinely by JAXA/EORC. Sea ice binary image derived from PALSAR data has originally the spatial resolution of 25m, because the scattering entropy is calculated in the area of 8 pixels in azimuth by 4 pixels in range direction on level 1.1 data. Since AMSR-E sea ice concentration (L2) is 10.0km, which is 400 times as large as that of PALSAR, there is a big difference in spatial resolution of sea ice concentrations derived from PALSAR and AMSR-E data. The number of sea ice pixels within 10 km squared area were counted and converted to PALSAR sea ice concentration.

The comparison of sea ice concentration between PALSAR and AMSR-E is given in Fig. 5. Although the consistency in derived sea ice concentration is about 60 percent, we found some differences especially in AMSR-E low concentration area.

5.2 Time difference between PALSAR and AMSR-E observation

Since the sea ice in our test site is usually drifted, it is assumed that the time difference between PALSAR and AMSR-E observations causes some errors in Fig. 5. We investigated the influence of time difference between PALSAR and AMSR-E observations by analyzing the daily averaged AMSR-E sea ice concentration as well as the nearest orbit sea ice concentration. Since the analyzed results did not have significant difference between two cases, it was concluded that the difference of sea ice concentration between PALSAR and AMSR-E was not caused by observation time difference.

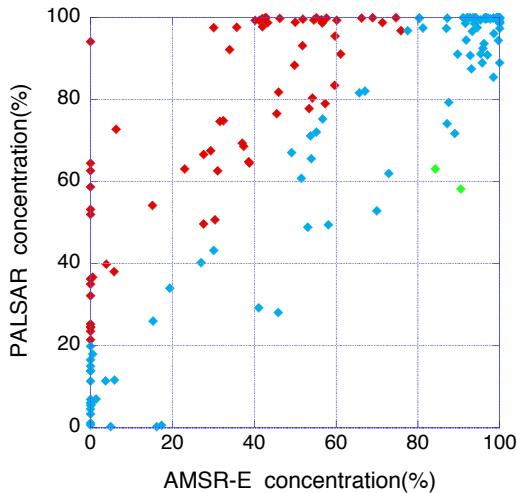
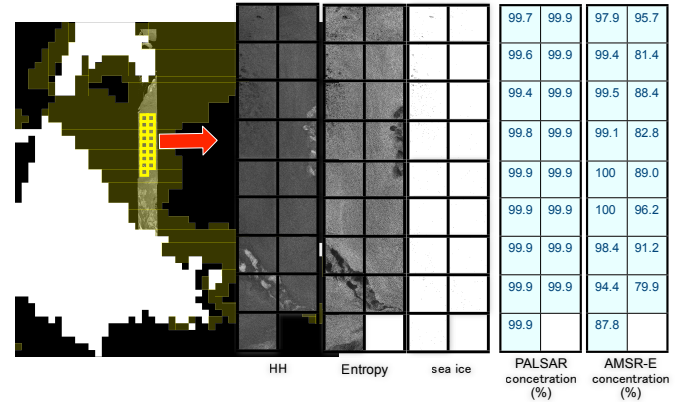


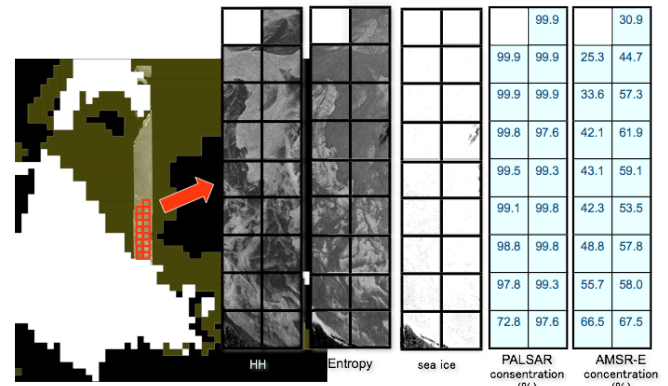
Fig.5 Comparison between PALSAR and AMSR-E sea ice concentration.

5.3 Sea ice characteristics detected by PALSAR and AMSR-E

Our proposed method tends to overestimate sea ice concentration compared with AMSR-E data as shown in Fig. 5. Since the influence of the land to AMSR-E data gives higher sea ice concentration in the area close to land-ocean boundary, this cannot explain the difference between PALSAR and AMSR-E sea ice concentrations. We investigate the area where PALSAR overestimates in detail.



(a)



(b)

Fig. 6 Typical area where PALSAR overestimate sea ice concentration, which was acquired on Feb. 17, 2009.

(a) small difference (b) large difference

Fig. 6 shows two typical examples of area where the difference of sea ice concentration between PALSAR and AMSR-E is small and large, which were acquired on Feb. 17, 2009. Each figure includes HH backscattering coefficient, scattering entropy and the detected sea ice area with PALSAR and AMSR-E sea ice concentrations. In order to investigate the sea ice characteristics quantitatively for the area corresponding sea ice concentration differences, the relation between HH backscattering coefficient and scattering entropy was plotted as shown in Fig. 7. The

characteristics appeared on the area where PALSAR overestimates are typically low in backscattering coefficient and high in scattering entropy.

The sea ice of which thickness is less than 10 cm and no snow on the top shows the same characteristics according to our past research [4]. Since we can recognize sea ice cover in backscattering coefficient as well as scattering entropy in Fig. 6 and 7, we suppose that there must be the thin sea ice existing which AMSR-E cannot detect.

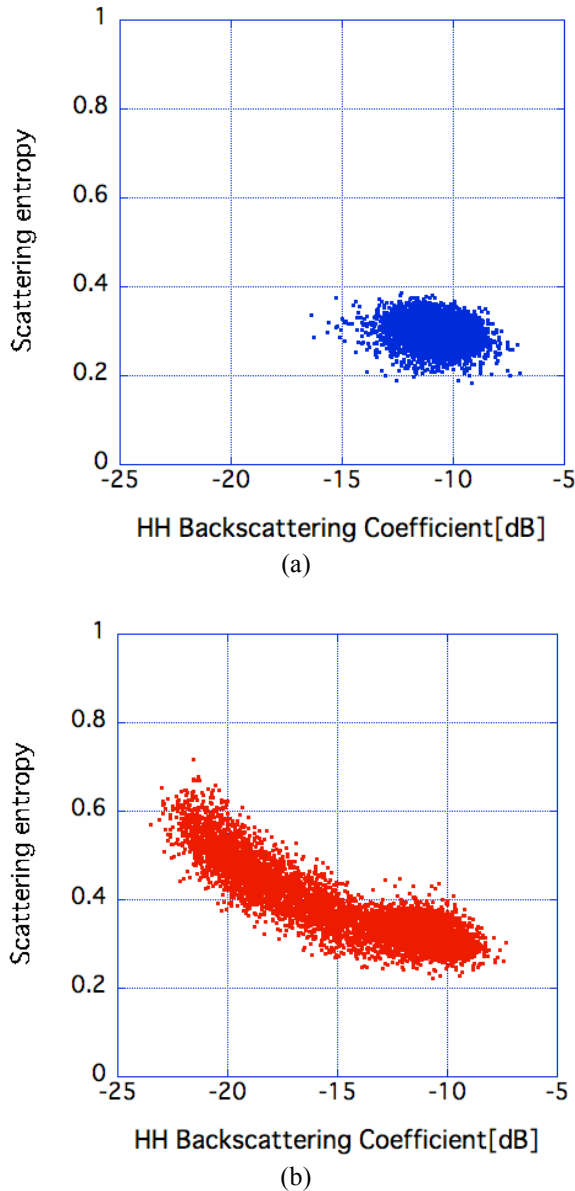


Fig.7 Scatter plot of the PALSAR HH backscattering coefficient and scattering entropy in sea ice area.
 (a)Area within 1% of sea ice concentration difference.
 (b)Area more than 60% of sea ice concentration difference.

5.4 Sea ice detection by MODIS data

MODIS visible channels were used to evaluate a reliability of our proposed method in sea ice detection. Only one dataset acquired in 2010 could be used for this analysis, because all other dataset had relatively high cloud coverage in our test site.

Fig. 8 shows the cutout MODIS data acquired on Feb.20, 2010. The PALSAR observed area on the same day was superimposed in the same figure. Fig. 8 clearly shows that we can compare two dataset for sea ice detection, although the time difference between MODIS and PALSAR observations is almost 8 hours.

Sea ice detection from MODIS data is based on the threshold in surface albedo calculated in visible wavelength. By combining MODIS 3 channels (band 1, 3, 4), an albedo A_v can be calculated as follows,

$$A_v = 0.3265 * B1 + 0.4364 * B3 + 0.2366 * B4 \quad (2)$$

where B1, B3, and B4 are the reflectance calculated from digital number in each channel. We also used band 7 (short wave infrared) data for making a mask image for the cloud area, and SRTM-3 data for making a mask image for land area. By using the threshold of albedo for detecting sea ice, sea ice area was classified into 3 categories, such as new ice, young ice and first-year ice [7]. Finally, a sea ice map with the spatial resolution of 500m was created.

Fig. 9 shows the comparison between the scattering entropy and MODIS albedo for the sea ice detected by our proposed method within the PALSAR observation swath. The spatial resolution used in this comparison was 500m.

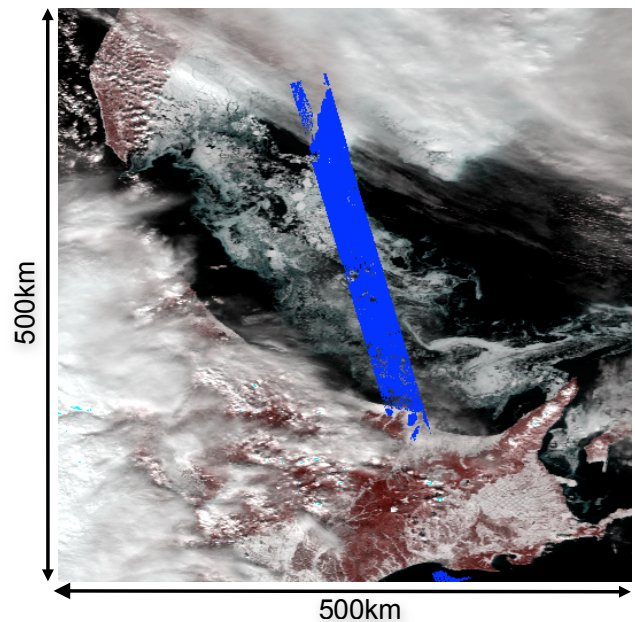


Fig.8 MODIS image acquired on Feb. 20, 2010. The extracted sea ice area from PALSAR data is overlaid.

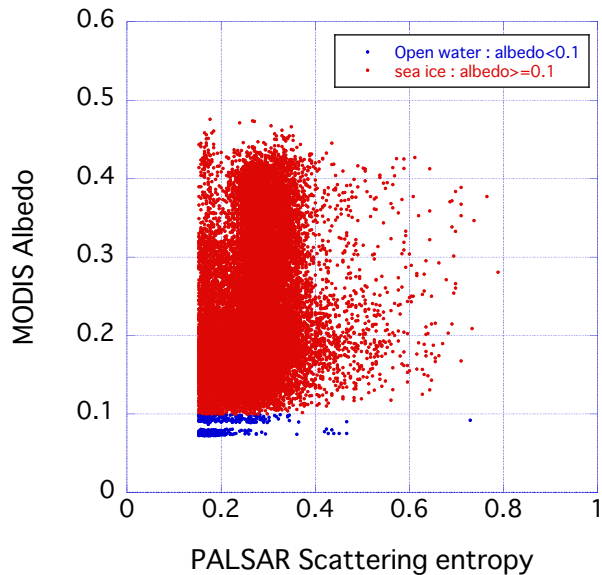


Fig.9 Comparison of PALSAR scattering entropy and MODIS albedo in sea ice area.

As the result, 96 percent of PALSAR detected sea ice area was also detected by MODIS data. Since MODIS albedo indicated less than 0.4 in the most of the sea ice area, the evaluated area is covered by new ice of which the thickness may be less than several 10 cm.

6. SUMMARY

A method to detect sea ice from PALSAR data was proposed and applied to relatively thin sea ice area in the Sea of Okhotsk. This method is based on the findings in our previous research that used the airborne L-band SAR data, in which the scattering entropy has consistently low in open water area.

The AMSR-E sea ice concentration was used to verify our proposed method. The difference in two sea ice concentrations was found especially in AMSR-E low concentration area. The high resolution backscattering and scattering entropy images give us an idea that there is some difficulty in AMSR-E to detect thin sea ice in the Sea of Okhotsk.

MODIS data were used to evaluate a reliability of our proposed method for sea ice detection. Since 96 percent of PALSAR detected sea ice area was also detected by MODIS data, we can conclude that our proposed method is reliable to detect thin sea ice area.

ACKNOWLEDGEMENT

This work is supported by KAKENHI (20651004), and conducted under the agreement of JAXA Research

Announcement titled "Sea ice study and its application using PALSAR polarimetric data in the Sea of Okhotsk (JAXA-PI: 205)". The PALSAR data are distributed under this agreement.

REFERENCES

- [1] F. Nishio and M. Aota: Variability of sea ice extent in the Okhotsk Sea. In 8th International Symposium on Sea Ice and the Sea of Okhotsk, 1--5 February 1993, Mombetsu, Japan. Proceedings. Mombetsu, Japan, Okhotsk Sea and Cold Ocean Research Association, pp.305-307, 1993.
- [2] T. Toyata, K. Baba, E. Hashiya, and K. I. Ohshima, "In-situ ice and meteorological observations in the southern Sea of Okhotsk in 2001 winter: Ice structure, snow on ice, surface temperature, and optical environments," *Polar Meteorol. Glaciol.*, vol. 16, pp. 116-132, 2002.
- [3] Onstott, R. G. 1992. SAR and Scatterometer Signatures of Sea Ice In: Carsey F. D. (editor). *Microwave Remote Sensing of Sea Ice (Geophysical Monograph 68)*. Washington, DC: American Geophysical Union : pp. 73-104.
- [4] H. Wakabayashi, T. Matsuoka, K. Nakamura and F. Nishio: Polarimetric characteristics of sea ice in the Sea of Okhotsk observed by airborne L-band SAR, *IEEE Trans. on Geo-science and Remote Sensing*, Vol. 42, No.11, pp. 2412-2425, 2004.
- [5] S.R.Cloude, and E. Pottier : A review of target decomposition theorem in radar polarimetry, *IEEE Trans. Geosci. Remote Sens.*, Vol. 34, No.2, pp. 498-518, 1996.
- [6] J. F.Heinrichs , D. J.Cavalieri, T. Markus : Assessment of the AMSR-E Sea Ice Concentration Product at the Ice Edge Using RADARSAT-1 and MODIS Imagery, *IEEE Trans. on Geo-science and Remote Sensing*, Vol.44, No.11, pp. 3070-3080, 2006.
- [7] D.K.Hall, D.J.Cavalieri, T.Markus: Assesment of AMSR-E Antarctic Winter Sea-Ice Concentrations Using Aqua MODIS *IEEE Trans. on Geo-science and Remote Sensing*. Vol.48, No.9, pp.3331-3339, 2010.